

Document downloaded from:

<http://hdl.handle.net/10251/95461>

This paper must be cited as:

Payri, R.; B Tormos; Gimeno, J.; Bracho Leon, G. (2011). Large Eddy Simulation for high pressure flows: Model extension for compressible liquids. *Mathematical and Computer Modelling*. 54(7):1725-1731. doi:10.1016/j.mcm.2010.12.001



The final publication is available at

<http://doi.org/10.1016/j.mcm.2010.12.001>

Copyright PERGAMON-ELSEVIER SCIENCE LTD

Additional Information

Large Eddy Simulation for high pressure flows: model extension for compressible liquids

R. Payri, B. Tormos, J. Gimeno¹, G. Bracho

*CMT - Motores Térmicos, Universidad Politécnica de Valencia
Edificio 6D, 46022, Valencia, Spain.*

Abstract

The present study gives a general outline for the fluid-dynamical calculation of flows at high pressure conditions. The main idea is to present a mathematical description of high pressure processes in liquids at compressible conditions, quantifying the effect of density variations on the flow pattern due to those pressure variations. The improved mathematical approach is coupled to a Large Eddy Simulation (LES) solver. The main code was developed by OpenSource Ltd for OpenFOAM, and the authors have introduced the additional expressions in order to calculate particular variables. For validating the code improvement, the LES solver is applied to a modern common-rail nozzle injector used in diesel engines. Results have been compared against other calculations that assumed constant properties and simultaneously validated with experimental data.

Keywords:

Large Eddy Simulation, Compressible, Liquids, Diesel injectors

¹ Corresponding author. Email: jaigigar@mot.upv.es

Cite as:

Payri R., Tormos, B., Gimeno, J., Bracho, G., “Large Eddy Simulation for high pressure flows: Model extension for compressible liquids”, *Mathematical and Computer Modelling*, (2011), Vol. 54 (7), pp. 1725–1731.
doi:10.1016/j.mcm.2010.12.001

Nomenclature

A	Area.
C_d	Discharge coefficient.
Co	Courant number.
F	Face Fluxes.
k_n	Fitting Constants.
\dot{M}	Momentum flux in axial direction.
\dot{m}	Mass flux.
\dot{m}_{th}	Theoretical Mass flux.
M	Mach number.
p	pressure.
Re	Reynolds number.
u	Velocity field.
u_{ef}	Effective Velocity.
T	Temperature.
t	time.
μ	Dynamic viscosity.
ρ	Fuel density.
τ	Sub-grid Scale Stress.

1. Introduction

The numerical approaches for solving the simplified Navier-Stokes equations for liquid flows are numerous. Most of the times, in the modelling of liquid flows at any pressure condition the density is considered as a constant. So far, this assumption was applicable for the majority of liquids flows present in the industry, where pressure and velocity values were moderate. Nevertheless, thanks to the technical improvements, nowadays, it is possible to achieve very high pressure conditions that produce flows with increased velocity profiles [1]; in some cases the speed is so elevated that Mach numbers could reach values higher than 0.3, so the liquid flow could become compressible, depending on pressure and density changes relative to the local speed of sound [2]. Usually, this kind of flows involves significant changes in density. Moreover, many authors have confirmed that density is a property that increases with pressure, therefore, density will increase when pressure is higher [3].

Besides, the high velocity values of the flow induce turbulent regimes, complicating the physics and the mathematical description of these processes. Many problems of practical engineering interest, such as aerodynamics, combustion and acoustics demand the modelling of turbulent compressible flows, so it is becoming an important aspect for calculations enhancement.

So far, the modeling technique available for solving turbulent flows with a reasonable accuracy – cost ratio is the Large Eddy Simulation (LES). However, they are developed mainly for incompressible flows ($\rho = \text{constant}$). Current LES softwares are not able to resolve the aforementioned problem for turbulent liquids at compressible conditions (for moderate Mach numbers), for this reason, the aim of this work is to improve a LES solver, extending the mathematical description of high pressure processes in liquids, considering density as a variable. An existent incompressible LES code for liquids has been modified in order to consider the influence of variable liquid density in the solved conservation equations.

For validating the code improvement, the modified LES solver is applied to a specific industrial process, such as modern common-rail nozzle injector used in diesel engines. Flow in diesel injection nozzles is characterized by high pressure drops that produce very high velocities. Therefore, because of the elevated pressure drop, density variations inside the domain could be very important, and this variation could modify the flow velocity and discharge coefficients. This paper is organised as follows, Section 2 presents the filtered Navier-Stokes equations and the computational procedure extension. After that, Section 3 describes the geometry and general setup of the cases used for validating the code improvement. Finally, results are presented and compared against other calculations that assumed constant properties, and simultaneously validated with experimental data.

2. Model Description

2.1. Mathematical Formulation

In this study a liquid flow with density variation is considered. The numerical simulation of the flow field has been carried out using LES, since it is able to reproduce the turbulence behaviour of the studied flow with high confidence and accuracy [4]. The basics of the LES Technique has been reported in several previous studies [5, 6]. The governing equations for flow field are the continuity and the momentum equations. Moreover, since

density is a variable, an equation of state is considered for the liquid, valid for high pressure conditions typical for this kind of flows.

Specifically, in this work the filtered continuity equation is written as:

$$\frac{\partial \rho}{\partial t} + \nabla \cdot (\rho \bar{u}) = 0 \quad (1)$$

where ρ is density, t is time and u is the velocity field. Commonly in liquid flows, when density is considered constant, the first term is neglected. But in this study since density is not constant, it should be taken into account. The overbar symbol represents the filtered variables [7]. The same operation is applied to momentum equation (Eq. 2). Again, density cannot be neglected in the left side of the expression and should be resolved.

$$\frac{\partial(\rho \bar{u})}{\partial t} + \nabla \cdot (\rho \bar{u} \bar{u}) = -\nabla \bar{p} + \mu \nabla^2 \bar{u} - \nabla \tau \quad (2)$$

In Eq. 2 μ is the dynamic viscosity of the fluid and τ is the Sub Grid Scale Stress. In order to estimate the sub-grid scale-stress the Smagorinsky model is used. This is one of the most convenient and widely used model in channels and internal flows [5, 8]. Moreover, for the wall damping it is used the Van Driest model. Details of the model have been performed and presented in [4].

In order to describe the effect of pressure on liquid density, appropriate equations of state should be considered. For the current study the equation of state derived by Payri et al. has been used [3]. They measured experimentally the variation of density for a wide range of pressures and many temperatures T . The pressure range considered by Payri et al. was from 25 MPa up to 180MPa, and the temperature was varied from 293 K to 348 K [3]. They performed the measurements for three different fuels, obtaining an empirical expression (Eq. 3). In this study it has been used the equation of state for the referred ‘Arct’fuel.

$$\rho = k_1 + k_2 T + k_3 p + k_4 p^2 + k_5 T^2 + k_6 p T \quad (3)$$

In Eq. 3 density is calculated using a 2^{nd} order polynomial function of p , T and fitting constants k_n reported in [3], where the first three terms are the most significant. The advantage of using this simple expression is that it facilitates the coupling in the improved solver, avoiding a big increase in the computational time. Although density is a variable that also changes

with the temperature, for this study it is kept constant, then calculations are performed as isothermal conditions. One of the reasons for this consideration is to avoid the incorporation of the energy equation, which takes into account other variables such as enthalpy and specific heat capacities, that are not well defined for liquids at high pressure values. Nevertheless, future works will try to define a relation for solving these equations considering the temperature variations.

The aforementioned equations have been inserted to a standard *LES* solver existent for incompressible flows. It is available in the software OpenFOAM, which is a flexible software that allows to incorporate more models and expressions. It is produced by *OpenCFD[®] Ltd*, is freely available and open source, licensed under the *GNU General Public License*. In detail the equations 1, 2 and 3 have been added to the existent code and the algorithm has been extended in order to solve them. Then, now the improved solver is able to calculate the flow for compressible liquids. The algorithm extension is explained in the following section.

2.2. Computational procedure

To numerically solve the equations presented in previous section (Eq. 1, 2 and 3), in this study the PISO (Pressure Implicit with Splitting of Operators) procedure proposed by Issa [9] is used, which couples the pressure to the velocity via flux conservation.

The procedure employed is the typical of any incompressible solver, but it is slightly modified. In detail, two more steps have been added to the algorithm. In the standard procedure, the first step of the solution cycle is to update the turbulent properties using the initial or previous time step values of u , p and face fluxes F . In this study, density value ρ is included in the updating. Subsequently, the momentum predictor step solves a tentative velocity using the old time values of p and F . For all the equations solved in the subsequent PISO steps, ρ is coupled. Then, for example, the ‘step’ that solves the momentum equation has included the density as a variable.

After that, due to the explicit nature of the non-orthogonal component of the face interpolation of p , the pressure equation has to be solved iteratively. Usually, a single or two corrector steps are enough to converge the non-orthogonal component [10]. In this study two correctors have been used.

The solution of pressure is followed by the projection of the velocities and fluxes into a divergence free form. After repeating previous steps iteratively until the dependent variables stop changing, another modification is done:

at the end of the loop, the density value is updated applying the equation of state (Eq. 3), using the final pressure values. Generally, the iterative process require less than three iterations, since time steps used in LES are very small. Finally, the calculation moves to the next time step, where actual values are used as initial parameters for the next cycle of the solution.

$$Co = \max \left(\frac{|u|}{\Delta x} \right) \Delta t \quad (4)$$

Concerning the time step, it was bounded by the Courant number Co , calculated as states Eq. 4. The maximum Co was limited to 0.4, therefore, the calculated time steps were around 1e-9 s, due to the high pressure drops that induced very high velocity. Also, the small cell size contributes to decrease the time step value.

3. Test Cases

3.1. Geometry description

As was commented before, for validating the code improvement, the modified LES solver is applied to a specific industrial process, such as modern common-rail nozzle injector used in diesel engines. That particular flow is under high pressure condition. Additionally, inside the nozzle the liquid experiences an expansion, producing significant gradients of the fuel properties. The study is focused just to the liquid phase inside the nozzle, and the main goal is to predict the flow pattern at the hole exit (velocity and discharge coefficients).

The orifice has an outlet diameter of 112 μm and 1 mm of length. The geometry corresponds to an axi-symmetric nozzle manufactured specially for research purposes. The orifice has a convergent shape, thus cavitation is avoided, so the simulation only involves incompressible liquid. The simulation conditions are characterized by a pressure inlet of 120 MPa and a pressure outlet of 5 MPa. Since the code assumes isothermal conditions, the temperature used for the simulations was 298 K. An additional reason for considering isothermal flow is due to the lack of knowledge of the real temperature distribution inside the injector nozzle, given that it is a very transient flow that difficulties the experimental measurements. The operating pressure condition is selected due to the existence of previous experimental data [11], so comparison and validations can be made. The fluid is winter diesel fuel, used in experimental works mentioned previously. The fluid viscosity used in

the simulations is $2.68e-3$ Kg/m.s, whereas the density has been calculated from pressure values, according the state equation presented before (Eq. 3).

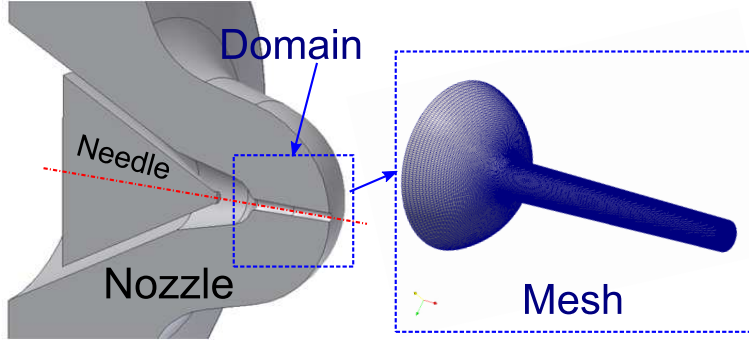


Figure 1: Nozzle geometry used for the simulations. Computational domain and mesh of the simulated volume

In Figure 1, it can be seen the characteristics of the computational mesh constructed for testing the new LES solver ability. The mesh is constructed from hexahedron cell shapes. The mesh near the wall has been refined obtaining a mesh resolution of $0.05 \mu\text{m}$ at the hole exit section; also, the mesh size is around 1.5 million cells. Moreover, previous grid study has been carried out and presented in [12].

3.2. Boundary conditions

In order to reproduce real physical conditions with fidelity, the boundary conditions should be defined carefully because they affect directly the flow, consequently the results. The boundary conditions settled for these calculations are:

- Inlet: Uniform pressure condition was used, and zero gradient velocity setup. In this study, the mapped method proposed by other authors was not necessary [13], and the inlet uniform pressure used was the corresponding pressure at this section when the pressure upstream is equal to 120MPa (in the injector entrance).
- Outlet: Uniform pressure condition was used, and zero gradient velocity setup. The fact of using pressure boundary conditions instead of velocity boundary conditions, could deteriorate the stability of the calculation [7]; but they are closer to the real physics of the problem. The

Table 1: Case description

Case Name	Solver	Pinlet [MPa]	Poutlet [MPa]
Case1	Improved code	120	5
Case2	Standard code	120	5

stability worsen was avoided releasing some limits of the calculation schemes.

- Walls: non-slip velocity condition.

3.3. Cases

The CFD code used for performing the simulations is OpenFOAM [14]. The case is solved twice: the first case has been calculated with the improved LES solver, named in this study as *Case1*. The second case has been calculated with the standard incompressible LES solver, available in [14] and described in [4], and named in this work as *Case2*. Both cases were performed at same conditions. Details of the cases performed can be found in Table 1

4. Results and Validation

As previously mentioned, the improved code is used for predict the flow of a diesel nozzle injector. In this section the main results for the simulated cases are presented and analysed. Specifically, the results presented are Velocity trend along the nozzle domain, comparing *Case1* solved with improved LES code versus *Case2* solved with standard solver, analysing instantaneous and time-averaged velocity. These results will be validated using experimental data, comparing effective velocities and discharge coefficient values.

Figure 2 depicts a comparison between Case1 and Case2; where velocity contours are shown in the left side. The upper part depicts the improved solver case, whereas the bottom part presents Case2. Both cases fully assess the feasibility of the code for turbulent prediction of the flow, since small irregular structures appear in the velocity contours, then turbulent assumptions of the model work properly. However, it can be seen that velocity values are not exactly the same. Case solved with standard solver has slightly higher maximum velocities. This implies an over-prediction of the averaged

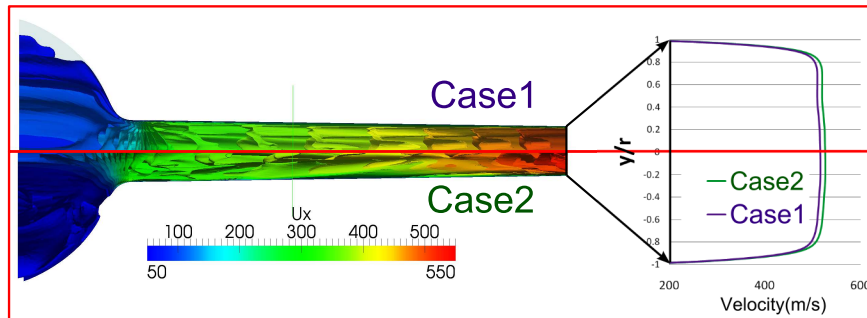


Figure 2: Velocity trend comparison. Instantaneous velocity is shown in the Left Side: *Case1* is depicted in the upper part, *Case2* is depicted in bottom part. The right side shows the Averaged Velocity profile in the exit section

velocities as will be demonstrated later on. In the right side of Figure 2 the streamwise time-averaged velocity at the hole exit is depicted. The vertical axis represents the radial position normalised by the hole radius, and the horizontal axis contains the velocity values. Case1 is depicted in purple line and Case2 in green line. The exit velocity profiles have very similar trend, also in the viscous layer, but higher maximum value is obtained for the standard code case. This will lead to higher mass flow prediction.

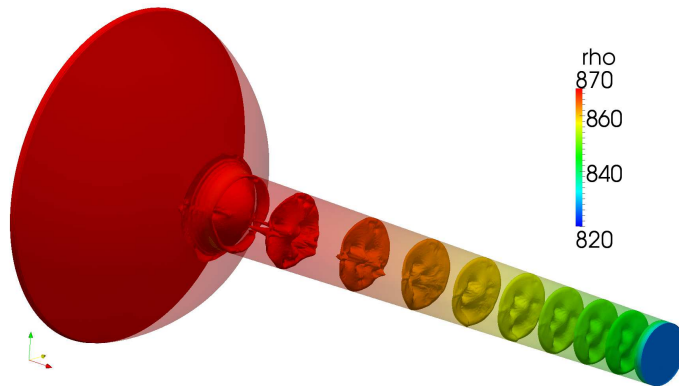


Figure 3: Instantaneous density contours.

Since the improved solver could calculate the density changes along the geometry, it is possible to visualise the density variation through the nozzle, depicted in Figure 3. As expected, higher density is obtained in the inlet zone, where pressure is higher, and it decreases gradually along the nozzle until

the hole exit. It should be noticed that this density variation is for constant temperature and certainly it may vary if temperature changes. Nevertheless, the temperature fluctuations in the domain are expected to be very small (in relation to the pressure drop) due to the transient behaviour of this particular flow. Besides, density values are smaller in the hole inlet radius (zones with very high pressure drops). This density profile information could be very useful for other future works involved with non-convergent nozzles, where cavitation usually appears [15].

As was commented before, simulated cases are validated against equivalent experimental results reported in [11]. Specifically, all the experimental data are time-averaged values of mass flow \dot{m} and momentum flux \dot{M} at the exit section of the hole; this means that the transient behaviour of the injection process is neglected. The parameters \dot{m} and \dot{M} were obtained using special devices, explained in detail in that work. With those variables it was possible to calculate the effective velocity u_{ef} at the hole exit using the following equations 5, 6, 7:

$$\dot{m} = \int_A \rho u dA \quad (5)$$

$$\dot{M} = \int_A \rho u^2 dA \quad (6)$$

$$u_{ef} = \frac{\dot{M}}{\dot{m}} \quad (7)$$

In analogy, \dot{m} , \dot{M} and u_{ef} were obtained from the simulated results applying the same equations through the section area at the hole exit domain. The first parameter used for comparison purposes is u_{ef} . The main reason for using effective velocity is the fact that it does not depend on the outlet diameter, and therefore possible errors due to differences between real nozzle diameter and simulated one are avoided. The comparison between the experimental and simulated effective velocity is depicted in Figure 4. As it can be seen, both cases over-predict the effective velocity, nevertheless the result obtained with the improved solver is much closer to the experimental value. The deviation related to the experimental value is not so high for the two cases, being *Case1* the closest to the experimental, with an error of around two percent.

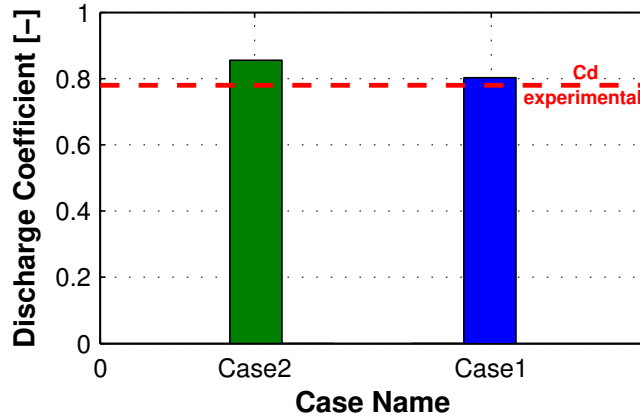


Figure 4: Effective Velocity Comparison: CFD values vs Experimental.

In addition, with the aforementioned parameters is possible to calculate the discharge coefficient C_d dividing the obtained mass flow \dot{m} by the theoretical mass flow \dot{m}_{th} , as states Equation 8:

$$C_d = \frac{\dot{m}}{\dot{m}_{th}} \quad (8)$$

Figure 5 plotted the experimental C_d in red line and the C_d calculated with both solvers. The result obtained with the improved solver (*Case1*) is closer to the experimental value, whereas the standard incompressible solver case over-predicts the result. This means that the improved solver reproduces in an enhanced way the real physics of the problem. It demonstrates that the flow is somehow in a compressible state for the tested pressures, and that compressibility causes additional losses that reduce the discharge coefficient. This is also in agreement with Benedict [16], who states that C_d of compressible flows is smaller than C_d of incompressible flows for the same Reynolds number.

5. Conclusions

The present study gives a general outline for the fluid-dynamic calculation of liquid flows at high pressure conditions. This is achieved improving an existent incompressible LES solver. The new solver is capable for performing calculations at variable density conditions. Density is considered as a variable

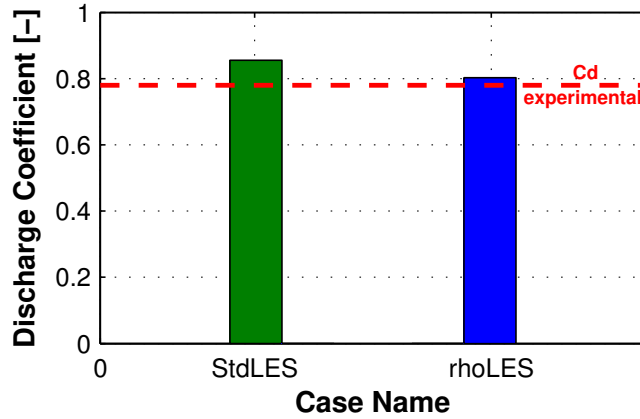


Figure 5: Discharge Coefficient Comparison: CFD values vs Experimental.

in all the equations, then improved solver determines density changes along the domain. Better prediction of velocity values at the hole exit is achieved, also there is an improvement in discharge coefficients determination (adapted to compressible conditions). The model could be customised in the future in order to consider the temperature fluctuations, applicable to other industrial validations. Nevertheless, compressible Solver is more expensive than the incompressible one, but it is capable to reproduce the flow pattern with enhanced precision.

Acknowledgements

This work has been funded by *MINISTERIO DE CIENCIA E INNOVACION* from Spain, in the framework of the project “ESTUDIO TEORICO EXPERIMENTAL DE LA INFLUENCIA DEL COMBUSTIBLE SOBRE LA CAVITACION Y EL DESARROLLO DEL CHORRO EVAPORATIVO”, Reference No. TRA2010-17564.

The authors would like to thank *Universidad de Valencia* for the computer resources, technical expertise, the assistance provided and for allowing the use of supercomputer *Tirant*.

References

- [1] H. Marzougui, H. Khlifi, B. Lili, Extension of the Launder, Reece and Rodi model on compressible homogeneous shear flow. The European

Physical Journal B 45 (2005) 147–154.

- [2] T.J. Chung, Computational Fluid Dynamics, Cambridge University Press, Cambridge, 2003.
- [3] R. Payri, F.J. Salvador, J. Gimeno, G. Bracho, The effect of temperature and pressure on thermodynamic properties of diesel and biodiesel fuels, *Fuel* (2010), doi:10.1016/j.fuel.2010.11.015.
- [4] R. Payri, B. Tormos, J. Gimeno, G. Bracho, The potential of large Eddy Simulation (LES) code for the modeling of flow in diesel injectors, *Mathematical and Computer Modelling* 52 (2010) 1151–1160.
- [5] U. Piomelli, Large-eddy simulation: achievements and challenges, *Progress in Aerospace Sciences* (1999) 335–362.
- [6] P. Sagaut, Large Eddy Simulation for incompressible flows. Springer, Berlin, 2001.
- [7] B. Vreman, B. Geurts, H. Kuerten, Subgrid-Modelling in LES of Compressible Flow, *Applied Scientific Research* 54 (1995) 191–203.
- [8] J.P. Roop, Numerical comparison of nonlinear subgridscale model via adaptative mesh refinement, *Mathematical and Computer Modelling* 46 (2007) 1487–1506.
- [9] R.I. Issa, Solution of the implicitly discretized fluid flow equations by operator splitting, *J. Computational Physics* 62 (1986) 40–65.
- [10] H. Seok-Choi, T. Seon-Park, K. Suzuki, Turbulent mixing of a passive scalar in confined multiple jet flows of a micro combustor, *International Journal of Heat and Mass Transfer* 51 (2008) 4276–4286.
- [11] R. Payri, F.J. Salvador, J. Gimeno, G. Bracho, Understanding diesel injection characteristics in winter conditions, SAE paper 2009-01-0836, 2009.
- [12] R. Payri, B. Tormos, J. Gimeno, G. Bracho, Internal flow modeling in diesel nozzles using Large Eddy Simulation, *Modelling for Medicine, Business and Engineering Congress*, 2009.

- [13] J. Jimenez, M.P. Simens, S. Hoyas, Y. Mizuno, Entry length requirements for direct simulations of turbulent boundary layers, Center for Turbulence Research - Annual Research Briefs, 2008.
- [14] OpenCFD Ltd., FOAM - The complete Guide, <http://www.opencfd.co.uk>
- [15] F.J. Salvador, J.V. Romero, M.D. Roselló, J. Martínez–López, Validation of a code for modeling cavitation phenomena in Diesel injector nozzles, *Mathematical and Computer Modelling* 52 (2010) 1123–1132.
- [16] R. Benedict, *Fundamentals of Temperature, pressure, and flow measurements*, Editorial John Wiley & Sons, New York, 1984.

Payri R., Tormos, B., Gimeno, J., Bracho, G., “Large Eddy Simulation for high pressure flows: Model extension for compressible liquids”, *Mathematical and Computer Modelling*, (2011), Vol. 54 (7), pp. 1725–1731.
doi:10.1016/j.mcm.2010.12.001